# DNA nanoparticles for ophthalmic drug delivery

de Vries, Jan Willem; Schnichels, Sven; Hurst, Jose; Strudel, Lisa; Gruszka, Agnieszka; Kwak, Minseok; Bartz-Schmidt, Karl-U.; Spitzer, Martin S.; Herrmann, Andreas

*Published in:*
Biomaterials

*DOI:*
10.1016/j.biomaterials.2017.11.046



*Publication date:*
2018

Biomaterials 157 (2018) 98–106

Contents lists available at ScienceDirect

Biomaterials

journal homepage: www.elsevier.com/locate/biomaterials

# DNA nanoparticles for ophthalmic drug delivery

Jan Willem de Vries [a, b, 2], Sven Schnichels [b, 2], José Hurst [b], Lisa Strudel [b], Agnieszka Gruszka [a, b], Minseok Kwak [a, c], Karl-U. Bartz-Schmidt [b], Martin S. Spitzer [b, d, *], Andreas Herrmann [a, **, 1]

[a] Department of Polymer Chemistry, Zernike Institute for Advanced Materials, University of Groningen, Nijenborgh 4, 9747 AG, Groningen, The Netherlands
[b] Centre for Ophthalmology, University Eye Hospital Tübingen, Elfriede-Aulhorn-Straße 7, D-72076, Tübingen, Germany
[c] Department of Chemistry, Pukyong National University, Busan, 608-737, South Korea
[d] Clinic for Ophthalmology, University Medical Center Hamburg-Eppendorf (UKE), Martinistr. 52, D-20246, Hamburg, Germany

ARTICLE INFO

*Article history:*
Received 18 September 2017
Received in revised form
14 November 2017
Accepted 27 November 2017
Available online 29 November 2017

*Keywords:*
DNA nanotechnology
Drug delivery
Ophthalmology
Nucleic acids
Nanoparticles

ABSTRACT

Nucleic acids represent very appealing building blocks for the construction of nano-scaled objects with great potential applications in the field of drug delivery where multifunctional nanoparticles (NPs) play a pivotal role. One opportunity for DNA nanotechnology lies in the treatment of ophthalmic diseases as the efficacy of eye drops is impaired by the short survival time of the drug on the eye surface. As a consequence, topical administration of ocular therapeutics requires high drug doses and frequent administration, still rarely providing high bioavailability. To overcome these shortcomings we introduce a novel and general carrier system that is based on DNA nanotechnology. Non-toxic, lipid-modified DNA strands (12mers with 4 lipid modified thymines at the 5′ end) form uniform NPs (micelles), which adhere to the corneal surface for extended periods of time. In a single self-assembly step they can be equipped with different drugs by hybridization with an aptamer. The long survival times of DNA NPs can be translated into improved efficacy. Their functionality was demonstrated in several ex-vivo experiments and in an in-vivo animal model. Finally, the NPs were confirmed to be applicable even for human tissue.



## 1. Introduction

In the last decades, rapidly advancing research in the field of DNA nanotechnology has resulted in a number of strategies to fabricate nucleic acid nanoarchitectures with well-defined sizes, periodicities and shapes in one-, two- and three dimensions [1–4]. Therefore, it is not surprising that this type of nano-scaled assemblies has attracted great interest from researchers working in the field of nanomedicine where well-defined multifunctional nanostructures are urgently needed. DNA nanoobjects can be exclusively self-assembled from nucleic acids by Watson-Crick base pairing and functionalization is achieved by hybridization with oligonucleotides. Examples are a DNA icosahedron functionalized with a target cell-recognizing aptamer or a 140 nm-long DNA tube, both loaded with anticancer drugs [5,6]. On the other hand, DNA strands can be chemically attached to a nanoscopic inorganic template and easily equipped with targeting units and drug molecules by hybridization with complementary oligonucleotide conjugates [7,8]. A similar type of nanoparticles for drug delivery was introduced by our group where the inorganic material is replaced by a soft matter core consisting of hydrophobic polymer units that are covalently attached to oligonucleotides to form DNA block copolymers [9]. So far, all DNA nanocarriers have been only applied for cancer therapy and proven functionality in vivo is very rare [10].

Currently, the vast majority of chronic and acute ocular diseases that are not managed surgically are treated using eye drops - a non-invasive mode of treatment that can be self-administered without medical supervision. However, only a small percentage of the active compound present in eye drops reaches its target tissue as it is rapidly cleared from the eye by tear fluid and eye lid movement [11,12]. As such, frequent administration of highly concentrated eye drops is necessary. Aside from the inefficiency of this dosage form,

* Corresponding author.
** Corresponding author.
*E-mail addresses:* martin.spitzer@med.uni-tuebingen.de (M.S. Spitzer), a.herrmann@rug.nl (A. Herrmann).
[1] Present address: DWI-Leibniz Institute for Interactive Materials, Forckenbeckstr. 50, 52056, Aachen, Germany and Institute of Technical and Macromolecular Chemistry, RWTH Aachen University, Worringerweg 2, 52074, Aachen, Germany.
[2] These authors contributed equally.

https://doi.org/10.1016/j.biomaterials.2017.11.046
0142-9612/

the requirement of frequent administration leads to poor compliance [13–15]. On the other hand, high concentrations of bioactive compounds produce side-effects that can range from simple irritations to, in extreme cases, a life threatening anaphylactic shock [16,17]. Thus, increasing the half-life of the drug on the eye is an important goal for more efficient treatment of eye diseases with fewer side effects.

The aim of this study is to overcome the limitations mentioned above, i.e. increase of adherence of the active pharmaceutically ingredient on the ocular surface, which improves drug action, with the help of a novel carrier system based on DNA nanotechnology. More specific, we address the most crucial parameters of a drug-delivery system: biosafety, compatibility with human tissue, the option to load different drugs, the functionality of the drug once released from the carrier and in-vivo efficacy. Therefore, we replaced the hydrophobic polymer unit of our DNA block copolymer delivery system [9] by several alkyl chain-modified 2′-deoxyuridine nucleotides (U) (Fig. 1a). When introduced into an aqueous environment, through microphase separation, DNA amphiphiles self-assemble into micellar nanoparticles (NPs) that exhibit a corona of single stranded DNA surrounding a lipid core [18]. Without any targeting unit, these NP adhere to corneal tissue for extended periods of time and they can be easily functionalized by a hybridization step. For imaging, we hybridized an oligonucleotide functionalized with a fluorophore onto the DNA carrier (Fig. 1b, top). To incorporate drug molecules, a DNA aptamer binding kanamycin B [19] and a RNA aptamer binding neomycin B [20] were extended at the 3′ end with the complementary sequence of the DNA amphiphile. Watson-Crick base pairing of aminoglycoside-complexed aptamers and DNA nanoparticles resulted in two antibiotic-loaded nanocarrier systems (Fig. 1b, bottom), proving the general drug loading strategy. Finally, with this nucleic acid based carrier platform we show that the long in vivo residence time of the nanoparticles on the cornea can be translated into improved efficiency in-vitro and in-vivo compared to the pristine drug, even demonstrating applicability with human tissue. To the best of our knowledge, it is the first time that nucleic acid-based carrier systems have been employed in the field of ophthalmology and that the adherence of DNA amphiphile NPs to corneal tissue has been shown.

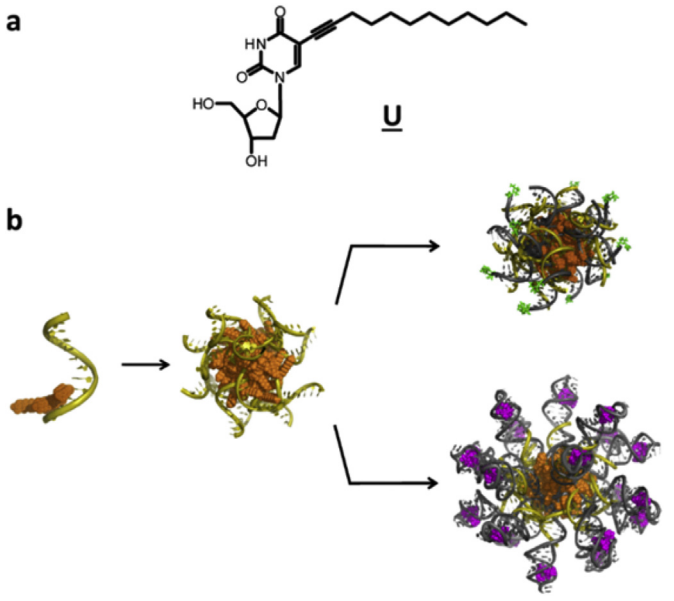


**Fig. 1.** Structure of lipid-modified nucleoside and functionalization strategy of DNA NPs used in this study. (a) Chemical structure of dodecyne-modified deoxyuracil, represented as U in the text. This nucleoside is incorporated into the oligonucleotide chain during DNA synthesis to impart hydrophobic properties. (b) The hydrophobic moiety attached to the nucleobase is shown in orange and the DNA is colored in yellow. In an aqueous environment, U-modified DNA strands self-assemble to form DNA nanoparticles due to their amphiphilic nature. The nanoparticles can then be functionalized through hybridization with a complementary DNA or RNA strand (grey). The functionality can either be covalently attached to the hybridized strands as realized for fluorescent dyes (green, top) or by non-covalent interactions employing an aptamer binding the drug molecules (purple, bottom). (For interpretation of the references to color in this figure legend, the reader is referred to the Web version of this article.)

## 2. Materials and methods

### 2.1. Synthesis and characterization of amphiphilic oligonucleotides

The modified 5-(dodec-1-ynyl)uracil phosphoramidite 3 was synthesized in two steps as previously reported in our group (Fig. S6) [21]. The modified uracil phosphoramidite was dissolved in $CH_3CN$ to adjust the concentration to 0.15 M, in the presence of 3 Å molecular sieves. The prepared solution was directly connected to the DNA synthesizer. All oligonucleotides were synthesized in 10 μmol scale on a DNA synthesizer using standard β-cyanoethyl-phosphoramidite coupling chemistry. Deprotection and cleavage from the PS support was carried out by incubation in concentrated aqueous ammonium hydroxide solution for 5 h at 55 °C. Following deprotection, the oligonucleotides were purified by using reverse-phase chromatography, using a C15 RESOURCE RPCTM 1 ml reverse phase column (GE Healthcare) through a custom gradients elution (A: 100 mM triethylammonium acetate (TEAAc) and 2.5% acetonitrile, B: 100 mM TEAAc and 65% acetonitrile). Fractions were desalted using centrifugal dialysis membranes (MWCO 3000, Sartorius Stedim). Oligonucleotide concentrations were determined by UV absorbance using extinction coefficients. Finally, the identity and purity of the oligonucleotides was confirmed by MALDI-TOF mass spectrometry and analytical anion exchange chromatography using a linear gradient elution, respectively (Figs. S7 and S8).

### 2.2. Preparation of nanoparticles

Nanoparticles were prepared in low bind tubes (Eppendorf) in 1× TAE buffer (10 mM Tris acetate, 0.2 mM EDTA, 20 mM NaCl, 12 mM $MgCl_2$, pH 8.0). Therefore, the lipid modified oligonucleotide of interest was prepared and one equivalent of the complementary DNA was added, ensuring a final concentration of 100 μM for each component. The micelles were formed and hybridized using a thermal gradient (90 °C, 30 min; −1 °C/2 min until RT). Afterwards, the NPs were diluted five times in ultrapure water and used as eye drops. When nanoparticles were used for fluorescence imaging a 5′ Atto488 functionalized complementary DNA was added to the lipid-DNA mixture.

Antibiotic loaded NPs were prepared at the needed concentration (20 μM) in 1× TAE buffer, no dilution was performed. For loading of neomycin B and kanamycin B a RNA and DNA aptamer were used, respectively [19,20]. Both were elongated with the complementary sequence of the carrier (Supplementary Table 1). For nanoparticle preparation, the lipid modified oligonucleotide and the complementary aptamer (1 molar equivalent) were loaded in a tube at the desired concentration and hybridized using a thermal gradient (85 °C, 30 min; −1 °C/2 min until RT). Subsequently, for neomycin B two equivalents of antibiotic per aptamer were added while for kanamycin B one equivalent per aptamer was used from a 10 mM stock solution in ultrapure water. The solution was incubated at RT for a minimum of 30 min and used without further dilution. When antibiotic loaded nanoparticles were used

for fluorescence imaging a 5′ Cy3 functionalized complementary DNA aptamer was used. Cy3 with an orange emission color was chosen in order not to confuse antibiotic loaded from unloaded NPs (Atto 488 has a green emission color).

### 2.3. Selection of best adhering NP and evaluation of adherence time on the cornea

Adult Lister-Hooded Rats were obtained from Charles River, Germany. Nanoparticles, prepared as described above, were administered to conscious rats at a concentration of 20 μM using a single drop of approximately 30 μl. For the eye drop applications the conscious rats were very shortly fixated and a drop was administered to the eye using a disposable dropping device as used in medical applications. Blinking of the eyes was not hindered during drop application or afterwards. After the designated incubation time-point, the rats were sacrificed with carbon dioxide inhalation. After sacrificing the animals, the eyes were enucleated and frozen in Tissue-Tek O.C.T. (Sakura Finetek, Germany) using liquid nitrogen. Frozen sections were longitudinally cut (12 μm) on a cryostat (Leica CM 1900, Germany), thaw-mounted onto glass slides (Superfrost plus, R. Langenbrinck Labor-und Medizintechnik, Germany) and stored at −30 °C until further use. For visualization, sections were fixed with methanol and to stain nuclei, sections were further incubated in a solution containing 0.2 μg/ml 4′,6-diamidino-2-phenylindol (DAPI) for 1 min. Stained sections were embedded in FluorSave (Calbiochem, Germany) and imaged using a fluorescence microscope (Axioplan2 imaging®, Zeiss, Germany with the Openlab software, Improvision, Germany) [22]. All animal experiments comply with the ARRIVE guidelines and were carried out in accordance with the U.K. Animals (Scientific Procedures) Act, 1986 and associated guidelines, EU Directive 2010/63/EU for animal experiments and the German animal protection law. The animal research was conducted under research permission AK3/11 granted by the Regierungspräsidium Tübingen to S. S.

### 2.4. Human cornea experiments

Five human cornea rims were kindly provided by the eye bank of the University Eye Hospital Tübingen after approval of the planned experiments. These rims are leftover tissue after a corneal transplantation. Informed consent was obtained from all human subjects. After the transplantation, the cornea rims were returned to the cornea media (KM1, Biochrom, Deutschland) until further use. Before applying the nanoparticles, the corneas were cut into 3–4 equal sized pieces, transferred to a 24-well plate and washed with PBS (PAA, Germany). Afterwards, 100 μl of the flouresence-labelled nanoparticles or buffer solution containing the fluorescence dye were applied on top of the cornea and incubated at room temperature for the designated time. Then the corneas were transferred to another well containing 2 ml of PBS and washed for the designated time at room temperature. Next the corneas were frozen in Tissue Tek, cut on a cryostat, stained with DAPI and photographed as described previously.

### 2.5. Evaluation of NP adherence by ocular fluorophotometry

Pig eyes were obtained from a local abattoir and washed before applying the NPs. To every eye 50 μl of NP solution (20 μM) was applied and the eyes were incubated for 5 min. Afterwards, excess liquid was removed and the fluorescence signal was measured on an Ocumetrics Fluorotron™ Master in triplo. Subsequently, the eyes were placed in 40 ml PBS and after the designated washing time the fluorescence was measured again. For each time point a minimum of three eyes were measured. For every eye three individual scans before application of the eye drops were taken to measure the background fluorescence. The average of the background was then subtracted from the average of every time-point measured afterwards. The percentages of every time-point in ratio to the instant measurement (immediate measurement after the drop was applied) are given. Data are represented as mean+/-SD. Statistical analysis was performed using JMP® (version 11.0.0, SAS Institute Inc.). ANOVA analysis with Tukey-Kramer post-hoc test was used for statistical evaluation of the individual time-points and the negative cornea samples (n = 3–11). Significances are indicated with * with $p < 0.05$, ** with $p < 0.01$ and *** with $p < 0.001$. Differences compared to Atto488 are shown with *, whereas comparison to U4T-Kan is indicated with +.

### 2.6. Evaluation of antibiotic activity on porcine cornea

Corneas were taken from porcine eyes obtained from the local abattoir and placed in a petridish. kanamycin B- or neomycin B-loaded NPs were prepared at a concentration of 100 μM as described above. A rubber ring was placed around the cornea to prevent spillage and 100 μl of NP or free antibiotic solution was placed on top of the cornea. After 5 min incubation time, extent liquid was removed or the cornea was washed in a large excess of PBS (typical volume 10 ml) for the designated time. Subsequently, the corneas were placed on petrifilms (3 M) prepared as recommended by the manufacturer. E. coli bacteria were grown at 37 °C overnight after which the amount of bacteria per ml LB medium was determined. Subsequently, the suspension was diluted to obtain a final concentration of $10^4$ E. coli/ml LB medium. On top of the corneas, on average 50 E. coli bacteria in 5 μl 1× LB medium were placed. For experiments with neomycin B, 0.5 mg/ml RNAse was added to the medium. The petrifilms were incubated at 37 °C for 48 h after which pictures were taken. The number of colonies was determined in duplo by three persons with the pictures being blinded. Data are represented as mean+/-SD. Statistical analysis was performed using JMP® (version 10.0.0, SAS Institute Inc.). ANOVA analysis with Tukey-Kramer post-hoc test was used for statistical evaluation of the individual time-points and the negative cornea samples (n = 3–4). Significances are indicated with *** and +++ $p < 0.001$.

### 2.7. Bactericidal effect on porcine cornea

Experiments were performed with *P. aeruginosa* obtained from ATCC (10145GFP™, LGC Standards GmbH, Germany). The clone is a descend from ATCC® 10145™, a neotype strain of *P. aeruginosa* [23], and contains a multicopy vector encoding the green fluorescent protein GFPmut3. Bacterial stocks were stored in 20% glycerol stocks at −80 °C. Bacteria were inoculated onto LB-Medium (agar 30 g/l, tryptone 10 g/l, yeast extract 10 g/l, pH = 7) containing Irgasan (Sigma-Aldrich, 25 mg/l) and incubated overnight at 37 °C. Bacteria were prepared at a concentration of ~$1 \times 10^8$ c.f.u./ml as determined by spectrophotometry ($OD_{600nm}$ = 0.8–1.0). For the experiment, corneas were taken from porcine eyes obtained from the local slaughterhouse and dissected with a tissue puncher and incubated with 40 μl of $10^8$ c.f.u./ml infectious *P. aeruginosa* bacteria solution for 15 min. After incubation each cornea was washed three times in 24 h with 0.5 ml PBS and afterwards supplemented with 0.3 ml DMEM. Kanamycin B-loaded NPs were prepared at a concentration of 500 μM using a similar procedure as described above. In short, the lipid modified oligonucleotide of interest was prepared at the desired concentration in 1× TAE buffer and hybridized using a thermal gradient (90 °C for 30 min; then −1 °C every 2 min until room temperature). Treatment was performed by incubating every cornea punch with 40 μl kanamycin-loaded NPs or kanamycin

alone, both at a concentration of 500 μM. The punches were incubated for 5 min with the solution and subsequently washed for 5 min with PBS. For the placebo control, the infected punches were incubated with buffer solution. Treatment was performed for 24 or 48 h. In the latter case the above described procedure was repeated a second time. Afterwards, the punches were shaken for 20 min at 24 °C in a thermomixer and serial dilutions (1:10) of the supernatants were incubated on PIA plates (Sigma-Aldrich, Germany). The number of colonies was determined by counting in duplicates. Data are represented as mean+/-SD. Statistical analysis was performed using GraphPad Prism 5 (GraphPad Software Inc. USA) ANOVA analysis with Tukey-Kramer post-hoc test of the individual timepoints and the placebo treated eyes (n = 5–6). Significances are indicated with *: $p < 0.05$; **: $p < 0.01$; ***$p < 0.001$.

### 2.8. In-vivo efficacy of kanamycin-loaded NPs

Experiments were performed with *P. aeruginosa* PA14 isolate, obtained from the laboratory of Dr. Sandra Schwarz from the Interfaculty Institute of Microbiology and Infection Medicine Tübingen [24]. The scarification murine models of infection was used as described previously [25,26]. Briefly, C57BL/6 J female mice (8–12 weeks old, Charles River, Germany) were anesthetized by intraperitoneal injection of a three-component anesthesia (0.005 mg/kg fentanyl, 2.0 mg/kg midazolam, 0.15 mg/kg medetomidine). Next, the eyes were damaged with a sterile 30-gauge needle, and 5 μl of the bacterial suspension (OD600 nm = 0.8–1.0) was pipetted directly onto the corneas and incubated for 15 min. Kanamycin B-loaded NPs were prepared at a concentration of 500 μM as described above. At 18 h after infection, the animals were examined, swabs were taken from every eye and spread on PIA plates to proof presence of bacteria. At this point also treatment with 5 μl kanamycin-loaded NPs (500 μM), kanamycin alone (500 μM) or kanamycin in clinical concentration (12.5 mM) was performed. The placebo group was treated with buffer solution. Mice were sacrificed 24 h after infection (6 h after treatment) and the eyes were enucleated, homogenized in 300 μl sterile PBS (pH 7.4) with a Precellys 24 homogenizer (bertin technologies, France). To determine the amount of viable bacteria, a 100 μl aliquot was serially diluted 1:10 in sterile PBS. Double aliquots (10 μl) of each dilution, were plated in duplicates onto PIA agar plates (Sigma Aldrich, Germany). Afterwards, the plates were incubated for 24 h at 37 °C before the number of colonies was determined. Treatment groups consisted of 4 mice, corresponding to 7–8 eyes. All animal experiments comply with the ARRIVE guidelines and were carried out in accordance with the U.K. Animals (Scientific Procedures) Act, 1986 and associated guidelines, EU Directive 2010/63/EU for animal experiments and the German animal protection law. The animal research was conducted under research permission AK1/15 granted by the Regierungspräsidium Tübingen to S. S. Data are represented as mean+/-SD. Statistical analysis was performed using GraphPad Prism 5 (GraphPad Software Inc., USA) ANOVA analysis with Tukey-Kramer post-hoc test of the individual treatment groups and the negative eyes (n = 7–8). Significances are indicated with *: $p < 0.05$; **: $p < 0.01$; ***$p < 0.001$.

## 3. Results

First, we investigated the effect of the structural features of the DNA nanoparticle components on the adherence of nanoobjects to the surface of the eye. Therefore, the corneal epithelium of living rats was exposed to different lipid-DNA nanoparticles. The following series of DNA amphiphile constructs was synthesized: U2-12, U4-12, U4-18, U6-12, U6-20, annotated as UX-Y, wherein X and Y represent the number of hydrophobic modified deoxyuridine bases and the total number of nucleotides, respectively (Fig. 2a). The very small NPs with diameters of around 10 nm (Fig. S1) are characterized by uniform size and exhibit critical micelle concentrations (CMCs) ranging from 4 to 27 μM (Fig. 2a and Fig. S2). They were hybridized with the fluorescently labelled complementary oligonucleotide to trace the localization in tissue slices. The eye drops containing the fluorescently labelled DNA amphiphiles at a concentration of 20 μM were administered to conscious rats using a single 30 μL drop. Control drops, containing single-stranded (ss) and double-stranded (ds) DNA with the same sequence and fluorescent label but lacking the hydrophobic modification were administered in the same way. Groups of animals were sacrificed 30 min, 2 h and 24 h after application. These time points were chosen for initial studies to cover both shorter as well as longer periods after installation. Cryosections of the treated eyes were visualized by fluorescence microscopy.

The best delivery system was determined as the NP carrier with the highest percentage of eyes exhibiting the DNA amphiphile and, in the case of similar results, by visual comparison of the cryosections (Fig. 2b and Fig. S3). Among the tested amphiphiles, U4-12 showed the best adherence to the corneal epithelium (Fig. 2c) while both ss and ds 12mer control sequences without any lipid modification did not show any affinity at all (Fig. 2d). From the results, we can deduce that the optimal ratio between standard and hydrophobic bases that promotes efficient adhesion is around 33% of modified content. NPs composed of ds oligonucleotides with lower (U2-12) or higher (U6-12) ratios exhibit significantly lower affinity. When comparing amphiphiles with similar percentages of U content (U4-12 and U6-20), strands with a smaller number of nucleotides showed better adherence. Therefore, both the number of lipid modifications and the total length of the amphiphile are important parameters determining adhesion to the cornea. Literature suggests several explanations for the observed affinity of the NPs. Either interactions of the NPs with the mucus layer [27,28] or with cell membranes, as shown for alkyl chain modified oligonucleotides previously [29,30], might explain the NP behavior on the ocular surface. The exact adhesion mechanism of the NPs is currently under investigation in our laboratory.

Before conducting further drug delivery experiments, the safety of the U4-12 NPs was determined using primary corneal epithelial cells. Three critical parameters -cell number, cell viability and apoptosis induction- were taken into account in evaluating biocompatibility (Fig. S4) [31,32]. The corneal cells were obtained from porcine corneas and incubated with DNA NPs at amphiphile concentrations of 20, 100 and 500 μM for 24 h. Although some effects of the NPs were significantly distinguishable from the cells treated with buffer, no disturbing effects were visible when maintaining a strict safety tolerance margin of 20%. In conclusion, the cells were incubated with the maximum concentration applied as eye drops (500 μM) for an extended time period and even then the NPs exhibit excellent biocompatibility indicating that they do not show toxic effects at these conditions. In the past, several promising nanoparticles used for drug delivery have been put aside due to toxicity of the carrier [33,34]. The absence of toxicity is thus an important finding and allows for further development of the U4-12 nanocarriers as an ocular drug delivery platform.

Upon the completion of proof-of-concept experiments and confirmation of the non-toxic nature of the NPs, we investigated aptamer-functionalized U4-12 carriers loaded with neomycin B and kanamycin B. Especially kanamycin B is widely used for treatment of ocular infections and can be anchored to a DNA NP via a well characterized high affinity aptamer [19,20]. To compare the time-dependent clearance of the antibiotic and the drug-loaded carrier, antibiotics were labelled with a green fluorescence dye (fluorescein) at one of the amine groups and the aptamer was

a

| Name | Sequence (5′ → 3′) | Lipid modified bases (# (%)) | CMC (μM) |
|---|---|---|---|
| U2-12 | UUTGGCGGATTC | 2 (17) | 27.4 |
| U4-12 | UUUUGCGGATTC | 4 (33) | 5.2 |
| U4-18 | UUUUGCGGATTCGTCTGC | 4 (22) | 4.6 |
| U6-12 | UUUUUUGGATTC | 6 (50) | 24.3 |
| U6-20 | UUUUUUGCGGATTCGTCTGC | 6 (30) | 4.2 |

b

| Time | U2-12 | U4-12 | U4-18 | U6-12 | U6-20 |
|---|---|---|---|---|---|
| 30 min | 2/4 | 6/6 | 3/5 | 3/4 | 4/4 |
| 2 hours | 0/4 | 4/6 | 0/4 | 0/4 | 2/4 |
| 24 hours | 0/4 | 0/4 | 0/4 | 0/4 | 0/4 |

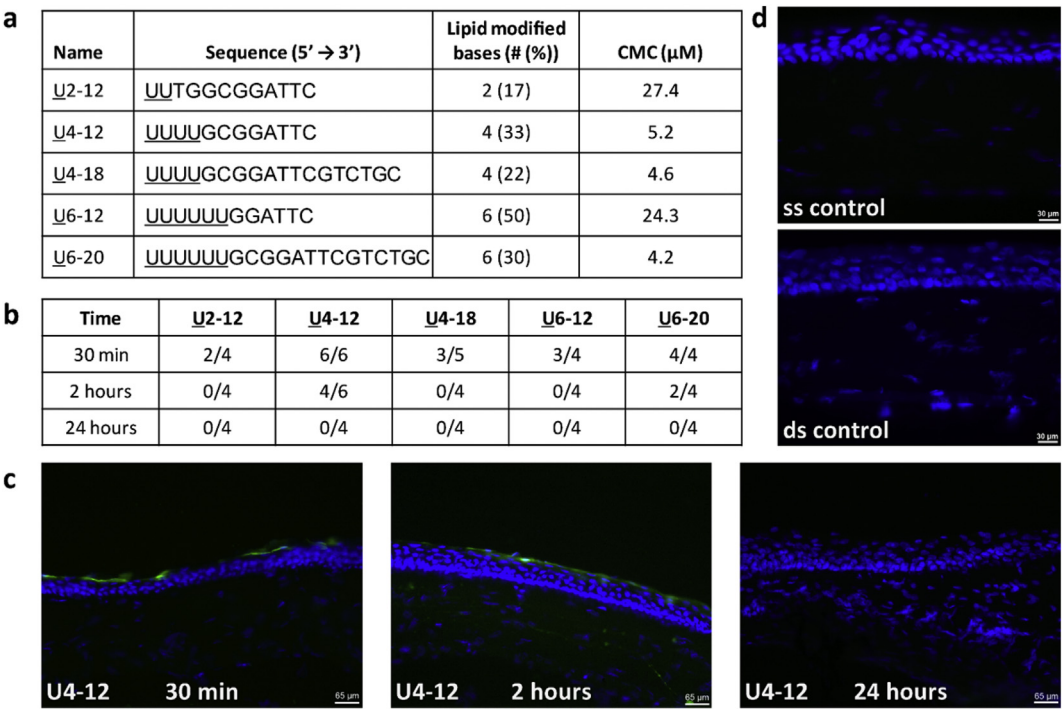


**Fig. 2.** Optimization of DNA NPs with respect to corneal adhesion. (a) Sequences and characteristics of lipid- modified oligonucleotides used to formulate NP-containing eye drops. (b) Overview of number of rat eyes tested positive for the presence of NPs out of total number of eyes to which the NPs were administered at various time points. (c) Fluorescence images of the adhesion of U4-12 NP (green) to the rat corneal epithelium (blue) at specific time points after eye drop administration. (For interpretation of the references to color in this figure legend, the reader is referred to the Web version of this article.)

functionalized with a red fluorescent dye (Cy3) at the 5′ end. Eye drops containing equal amounts of either NP-bound antibiotic or free antibiotic were administered to living rats as described earlier and the adherence to the cornea was studied 5, 15, 30 min as well as 1, 2 and 4 h after application (Fig. 3). Both neomycin B- and kanamycin B-loaded NPs are effectively attached to the cornea for a period of at least 2 h, whereas the fluorescent antibiotics are not detectable anymore after 5 min. These experiments indicate that adhesion to the cornea is enhanced by the carrier system, which allows the loading of different cargoes and their close contact to the corneal surface. It is important to mention in this context that the chemical structure of the drugs was not modified due to the non-covalent nature of NP loading. Since RNA and DNA aptamers are known to bind a large variety of molecular structures [35,36], these vehicles represent a general delivery platform for diseases of the anterior section of the eye that can be loaded with drugs in a modular fashion.

To demonstrate the translatability of this nanocarrier system from the rat model to the human model, we examined the adherence of antibiotic-loaded particles to human corneal tissue. The experiments were performed on discarded tissue from corneal transplantations. Eye drops containing nanoparticles were administered to the corneal epithelium, the tissue was incubated for 5 min and afterwards the cornea was washed. In consistence with previous experiments, fluorescently labelled antibiotics were used as control. Washing times after incubation were varied between 5 min and 2 h (Fig. 3). Both neomycin B- and kanamycin B-loaded NPs showed a remarkable attachment to the human cornea, while the free form of the drugs was displaced at the first time point investigated. A slow decrease in intensity accompanied increasing washing time for particles containing neomycin B. This can be due to detachment of the NPs from the corneal surface or because of degradation of the aptamer. In contrast, for kanamycin B this effect was not notable.

In a next step the adherence of the NPs was quantified. As the longest period after application at which the NPs were detected was 4 h, this point was selected as the last measurement. Since determination of the amount of carrier system is cumbersome using regular mass spectrometry, we employed ocular fluorophotometry to measure the amount of NPs present on the eye (Fig. 4). This method allows to accurately evaluate the amount of fluorescent probe present on the eye and is well established in the field of ophthalmology [37–41]. To this end porcine eyes were incubated with U4-12 NPs hybridized with the complementary strand bearing a fluorescent dye. For aptamer functionalized NPs, the fluorescently labelled kanamycin binding DNA aptamer was selected and hybridized on the pristine NPs. The free fluorophore was included as small molecule control. After 5 min of incubation, the fluorescence was measured and subsequently the eyes were washed for designated time periods. As is visible, 50% of the unfunctionalized NPs are retained after 5 min of washing. For this carrier, high fluorescence levels are observed even up to 4 h after washing, where still 28% of the initial value is measured. Also for the kanamycin binding carrier a high retention on the ocular surface is evident, with 20% of the initial fluorescence being present at the first time point. At 4 h washing 13% fluorescence is maintained. In contrast, the small molecule control is already washed out after 5 min. These results are in good agreement with the fluorescence microscopy studies shown above.

Next, we investigated whether an improved adherence half-life of the NPs translates into better activity and efficacy compared to the pristine drug. To do so, we first demonstrated that the antibiotic can be liberated from the NP by subjecting antibiotic-loaded NPs to a minimum inhibitory concentration test (MIC-test) using *Escherichia coli* (*E. coli*) (Fig. S5) and comparing the results to the free drug. To mimic nuclease containing body fluids on the ocular surface,

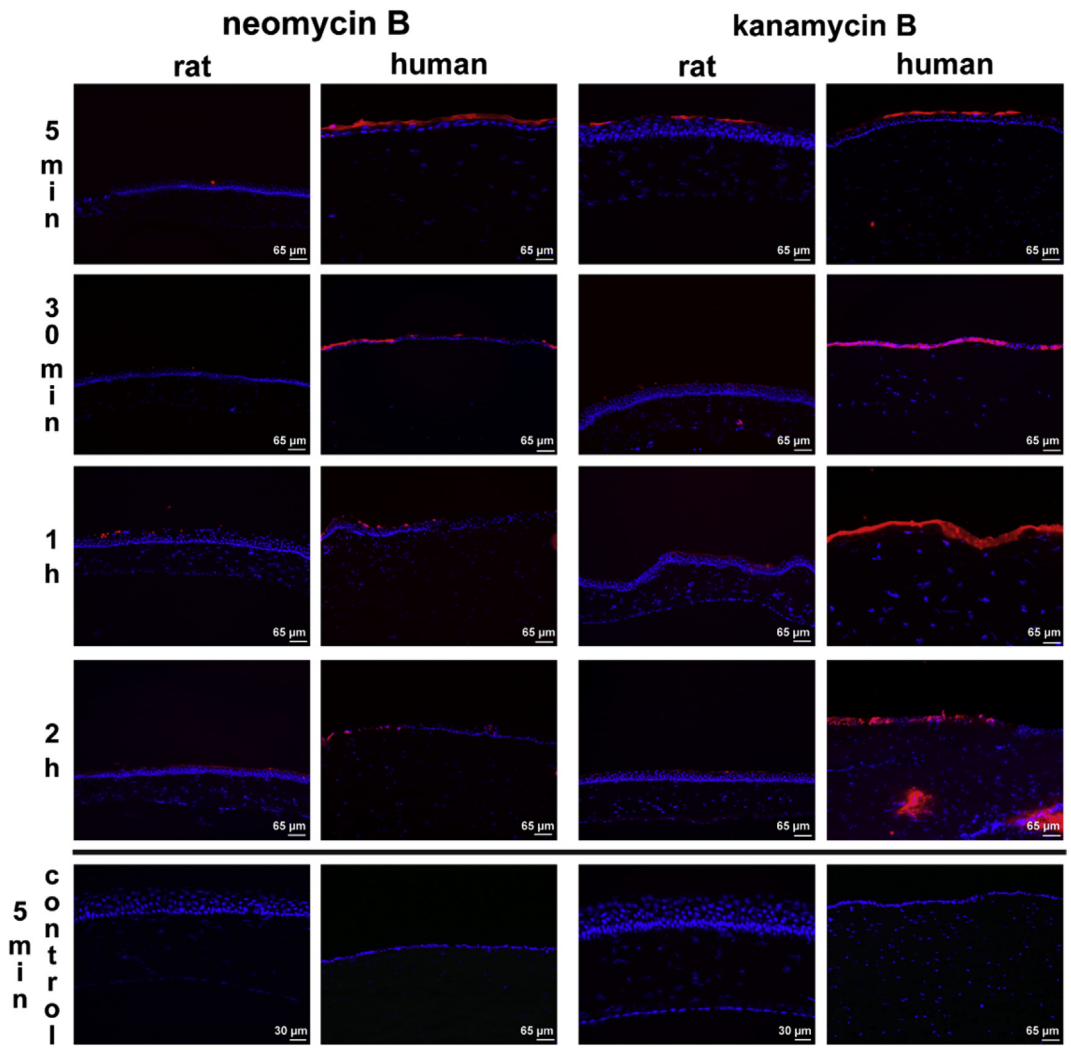


**Fig. 3.** Fluorescence images demonstrating adhesion of neomycin B- (left) and kanamycin B-loaded (right) NPs (red) to the rat and human cornea (blue). In the images in the bottom row, a fluorescently labelled form of the free neomycin B or kanamycin B was used as a control (green). The time point after administration of the AB-loaded NP or free AB is indicated on the left (n = 4–6 for rat eyes with NP, n = 2 for controls, n = 1 for human eyes). (For interpretation of the references to color in this figure legend, the reader is referred to the Web version of this article.)

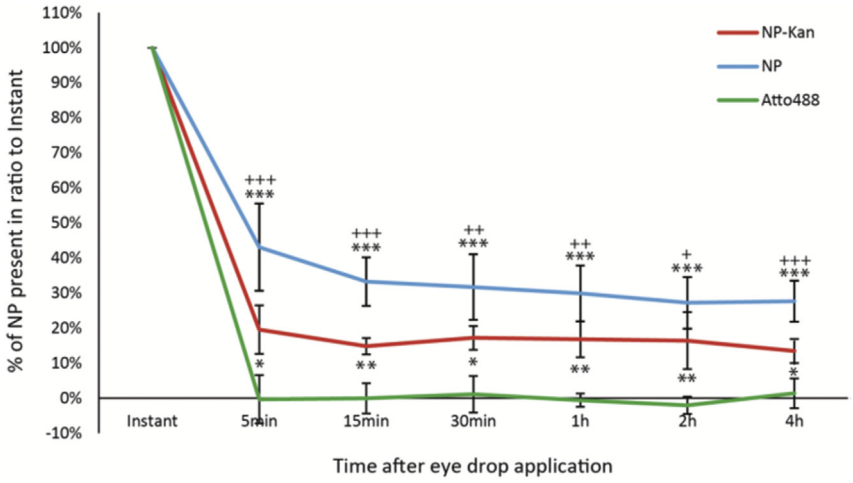


**Fig. 4.** Availability of NPs on the corneal surface determined by ocular fluorophotometry. The small molecule control is washed out already after 5 min whereas ds NPs with only fluorophore or functionalized with kanamycin binding aptamer show longer availability (n = 3–11). Statistical differences are shown as * with $p < 0.05$, ** with $p < 0.01$ and *** with $p < 0.001$. Differences compared to Atto488 are shown with *, whereas comparison to U4T-Kan is indicated with +.

RNAse and DNAse were added to the cell suspension containing neomycin B- and kanamycin B-loaded NPs, respectively. The bacterial growth was determined by measuring the optical density of the cell suspension at a wavelength of 600 nm after 5 h of incubation at 37 °C. The MIC tests clearly demonstrated that both nanocarrier-loaded antibiotics are active. Neomycin B-loaded NPs, however, required the presence of RNAse to release the drug and induce bactericidal effects while the presence of DNAse made little impact on the effectiveness of kanamycin B-loaded NPs. In the context of in-vivo applications, neither the RNAse-dependent release of the neomycin B nor the DNAse-independent release of the kanamycin B presents an obstacle because nucleases are prevalent in biological fluids [42].

Having demonstrated that the NPs exhibit excellent adhesive properties on the cornea and that the antibiotic activity is retained, we determined whether a clear antibiotic effect can be observed at the site of action. To this end, growth studies of *E. coli* were performed on porcine corneas where the efficacy of kanamycin-loaded NPs was compared to that of the free drug. Growth inhibition was first evaluated by incubating the cornea from porcine eyes with antibiotic-loaded NPs for 5 min. At the end of the incubation period, excess solution was removed. We simulate tearing by washing the porcine corneas with an excess of PBS buffer to evaluate the efficacy of the loaded NPs that are bound tightly to the cornea. The corneas were then placed on petrifilms containing growth medium and a total of on average 50 *E. coli* bacteria were applied to the cornea. After allowing them to grow for 48 h, the number of colonies was determined (Fig. 5a and b). The growth experiments clearly show the antibacterial activity after incubation of the cornea with free antibiotic. The antibiotics bound to the NPs showed similar growth inhibition, suggesting that the aptamers are degraded by nucleases or that the drugs are otherwise fully released from the NPs within the timeframe of the experiment. The results of the *E. coli* growth experiment on corneas washed for 5, 30 and 60 min after exposure to kanamycin B-loaded NPs illustrated one of the shortcomings of current ophthalmic medication. No significant growth inhibition is found for the free antibiotic after 5 min of washing, indicating that the drug molecule is washed away within this short timeframe. This is in good agreement with results from experiments where fluorescently labelled free antibiotics were not detected by fluorescence microscopy 5 min after application to the rat cornea in-vivo and the human cornea in-vitro. In contrast, the porcine corneas treated with the kanamycin B NPs exhibited bactericidal activity after up to 30 min of washing. Again, this is in good agreement with the extended NP adhesion time observed on the rat cornea.

In the next stage, a similar experiment was performed with the bacterial strain *Pseudomonas aeruginosa (P. aeruginosa).* This pathogen is highly infective and a common cause of bacterial keratitis, inflammation of the cornea [43,44]. To induce an ocular infection, ex-vivo porcine corneas were incubated for 15 min with the bacteria. Treatment was started 24 h afterwards and consisted of three times daily administration of 40 μl antibiotic-loaded NPs, free kanamycin or the buffer placebo for 5 min. Following the administration the eyes were washed for 5 min in PBS. This treatment was performed for one or two days in a row and afterwards the number of colonies was determined by incubation of the corneal extracts on selective growth plates (Fig. 5c). As evident from the growth study, after only one day of treatment the kanamycin-loaded NPs already greatly reduced the infection. This effect is maintained after the second day of treatment. In contrast, administration of the placebo results in an increase of the number of bacteria. In addition, the free antibiotic did not cause any significant growth reduction, again stressing the shortcomings of currently employed eye drop formulations.

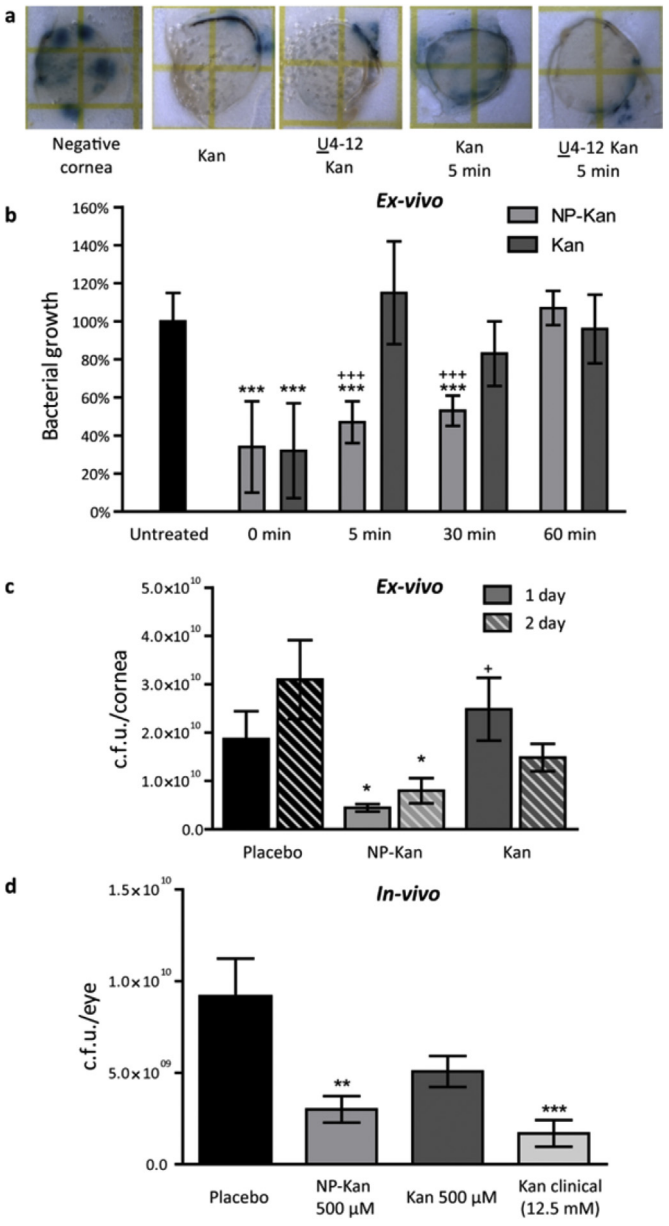


**Fig. 5.** Bacterial growth experiments with E. coli and *P. aeruginosa* on ex-vivo treated porcine corneas and in-vivo effectivity of kanamycin-loaded NPs in rats. (a) Representative photographs of E. coli growth with and without washing. (b) E. coli growth experiment with varying washing times (n = 3–4). Control (Negative cornea) is set to 100% growth. Statistical differences are shown as *** with $p < 0.001$ compared to untreated cornea. Comparison between kanamycin B and NP kanamycin B are shown as +++ with $p < 0.001$. Unmarked time points were not significantly different. Differences between the time-points were not evaluated. (c) *P. aeruginosa* survival after treatment with placebo (buffer only), kanamycin-loaded NPs, or the free antibiotic. Total amount of colony forming units (c.f.u.) per cornea was determined by growing extracted bacteria on selective agar (n = 5–6). Statistical differences are shown as * with $p < 0.05$ compared to placebo treated corneas at the same time point. Comparison between kanamycin B and U4-12 kanamycin B are shown as + with $p < 0.05$. Unmarked time-points were not significantly different. (d) In-vivo comparison of bactericidal effect on *P. aeruginosa* of placebo, kanamycin B-loaded NPs at a concentration of 500 μM, pristine kanamycin at 500 μM and clinically dosed kanamycin B at a concentration of 12.5 mM, showing significant effects for NPs and clinical kanamycin. Total amount of colony forming units (c.f.u.) per cornea was determined by growing extracted bacteria on selective agar (n = 7–8). Statistical differences are shown as ** with $p < 0.01$ and *** with $p < 0.001$ compared to placebo treated animals. Unmarked time points were not significantly different.

Finally, to proof in-vivo efficacy of our NP-carrier system, corneas of mice were also exposed to *P. aeruginosa* to induce a keratitis.

After confirming the corneal keratitis, the animals were treated with either placebo, free kanamycin or kanamycin loaded NPs. For the latter two, an antibiotic concentration of 500 μM was chosen. Additionally, the clinical formulation (12.5 mM) of kanamycin was used for treatment. To determine the amount of bacteria on the cornea, the animals were sacrificed and afterwards the eyes were enucleated and homogenized. The homogenized eye extracts were then serially diluted, grown on selective growth plates and the number of colonies was determined (Fig. 5d). As can be seen, also in the in-vivo setting the antibiotic-loaded NPs had a clearly significant bactericidal effect. The observed growth inhibition is similar to the clinically used kanamycin drops. It must be noted here that the latter formulation contains the antibiotic at a concentration of 12.5 mM, which is 25 times higher than employed for the NP bound drug. Similar to the ex-vivo experiments, the pristine kanamycin at the same concentration as the NPs does not induce a significant growth inhibition. These experiments proof that the long adherence time of the NPs can be directly translated into an in-vivo therapeutic effect.

## 4. Discussion

Treatment of eye diseases by eye drops is complicated due to several problems and improving efficacy of eye drops has been an important goal for many years [45]. By increasing the exposure time of the target tissue to the active compound in the drops, less frequent administration of less concentrated drops would be required. As a consequence, improved compliance is to be expected alongside lower levels of side effects. Moreover, ocular drug delivery systems provide the opportunity to administer medication that is toxic at the concentrations currently required [46].

To address these challenges several solutions have been brought up such as microparticles, in-situ gelling formulations, mucoadhesive polymers and ointments. Although these carriers have increased the half-life time of the drug on the eye to a certain extent, they do not offer sufficient effect and often cause a blurred vision or other side effects. Nanotechnological approaches have been pursued to improve bioavailability of medication on the ocular surface [45,47]. Of special interest are polymeric nanoparticles that adhere to the cornea and increase the bioavailability of the released drug. Although satisfactory effectiveness has been demonstrated in vitro and in vivo, these delivery vehicles still face several shortcomings [48–50]. The nanoparticles are characterized by a broad size distribution, easily exceed sizes of 100 nm and their composition needs to be greatly varied to accommodate drugs with different physicochemical properties.

One striking feature of this work is that it is one of the few studies, in which NPs were applied in a pathogenic model and -most importantly- superior efficacy compared to the pristine drug was proven. Most studies with other NPs were performed with healthy eyes showing adherence and delivery mediated by the carrier but not better efficacy [45]. With the herein presented NP systems, a better efficacy was proven with two pathogenic agents in-vitro and one common keratitis causing bacteria strain in an in-vivo set-up.

Our NP system offers more advantages compared to other drug carriers. For example many liposomes have the tendency to lead to blurry vision due to their large size [51]. It is well known, that blurry vision heavily reduces compliance, which is a major reason why ointments are not used for eye-care during the day or even at all. The benefit of the here presented NPs is that no blurry vision after implementation of the nanocarriers is observed, as they have an approximate diameter of 12 nm and their buffer solution is clear.

Regarding toxicity, only little work has for example been published regarding the toxicity of dendrimers, offering unsatisfactory results. Many other developed drug-delivery systems based on NPs (mainly synthetic polymer constructs) either directly showed toxicity or their degradation products were toxic [33,34]. The here presented DNA-NPs revealed an excellent biosafety profile in-vitro. As DNA is a natural biomacromolecule, no toxic effects are to be expected from degradation products in contrast to synthetic polymer NPs. The body-own DNAses in the tear fluid readily degrade the short DNA strands of the NPs without any residual components [42]. However, as biocompatibility and −saftey are a major showstopper for most drugs and -delivery systems, further experiments including long-term in-vivo experiments are running, which will be presented in a separate publication.

Last but not least, it needs to be mentioned that the here presented DNA-NP are not drug specific but multifunctional. They can bind lipophilic as well as hydrophilic drugs or reagents via different loading strategies. This is a major advantage over other drug-delivery systems, which are often limited by their chemical properties to a specific group of drugs [45]. Moreover, with different loading strategies several drugs may be incorporated into the same carrier, offering the opportunity to deliver hydrophobic and hydrophilic drugs with the same eye drop.

## 5. Conclusion

Here, we introduced a novel, powerful and general approach for treating eye infections using DNA nanotechnology that can be easily extended to treat other ocular indications as aptamers can be evolved against molecules with very diverse structures. We demonstrated functionalization of the DNA carrier with therapeutically active agents, i.e. the aminoglycoside antibiotics neomycin B and kanamycin B, imaging units (two fluorophores) or a combination of the two by simple mixing of components and hybridization to generate multifunctional nanoobjects. The NPs exhibited an excellent safety profile at the measured concentration against primary corneal epithelial cells. Without any targeting unit, they adhered for few hours to the cornea in living animals and human tissue and therefore dramatically increase the adherence time of the drug cargo. To the best of our knowledge, this is the first report describing the use of DNA-based carrier systems in the field of ophthalmic drug delivery. Furthermore, antibiotic-loaded NPs are proven to be more effective than free antibiotics in preventing bacterial growth on porcine corneal tissue under conditions simulating tear fluid production and especially on infected corneas in in-vivo experiments. Further studies of safety, stability, the adhesion mechanism and controlled drug release are currently under investigation and will be the subject of upcoming publications. These findings open a variety of possibilities for utilization of DNA-based materials in ophthalmic drug delivery.

## Author contributions

Research was conducted by J.W.d.V., S.S., L.S., J.H., M.K. and A.G. under guidance of M.S.S., K.U.B.S. and A.H. The manuscript was written by J.W.d.V., S.S. and A.H.

## Funding

This work was supported by an ERC starting grant from the European Commission (A.H.). A.H. also greatly acknowledges financial support from NWO (Vici grant and ChemThem grant) and the Zernike Institute for Advanced Materials. J.H. greatly acknowledges financial support from the Ernst-und-Berta-Grimmke Stiftung.

## Acknowledgement

We thank Johanna Wude and Katharina Frößl for their assistance. We thank the cornea bank in Tübingen for providing human corneal tissue. The authors greatly acknowledge the University Eye Hospital Tübingen for their support. We thank Dr. Sandra Schwarz and Dr. Annika Schmidt for providing the *Pseudomonas aeruginosa*.

## Appendix A. Supplementary data

Supplementary data related to this article can be found at https://doi.org/10.1016/j.biomaterials.2017.11.046.

## References

[1] J. Chen, N.C. Seeman, Nature 350 (1991) 631–633.
[2] P.W.K. Rothemund, Nature 440 (2006) 297–302.
[3] E.S. Andersen, M. Dong, M.M. Nielsen, K. Jahn, R. Subramani, W. Mamdouh, M.M. Golas, B. Sander, H. Stark, C.L.P. Oliveira, J.S. Pedersen, V. Birkedal, F. Besenbacher, K.V. Gothelf, J. Kjems, Nature 459 (2009) 73–75.
[4] J.C. Mitchell, J.R. Harris, J. Malo, J. Bath, A.J. Turberfield, J. Am. Chem. Soc. 126 (2004) 16342–16343.
[5] M. Chang, C.S. Yang, D.M. Huang, ACS Nano 5 (2011) 6156–6163.
[6] Y.X. Zhao, A. Shaw, X.H. Zeng, E. Benson, A.M. Nystrom, B. Hogberg, ACS Nano 6 (2012) 8684–8691.
[7] S. Dhar, W.L. Daniel, D.A. Giljohann, C.A. Mirkin, S.J. Lippard, J. Am. Chem. Soc. 131 (2009) 14652–14653.
[8] K. Zhang, L.L. Hao, S.J. Hurst, C.A. Mirkin, J. Am. Chem. Soc. 134 (2012) 16488–16491.
[9] F.E. Alemdaroglu, N.C. Alemdaroglu, P. Langguth, A. Herrmann, Adv. Mater. 20 (2008) 899–902.
[10] Z.Y. Xiao, C.W. Ji, J.J. Shi, E.M. Pridgen, J. Frieder, J. Wu, O.C. Farokhzad, Angew. Chem. Int. Ed. 51 (2012) 11853–11857.
[11] A.C. Amrite, H.F. Edelhauser, U.B. Kompella, Invest. Ophthalmol. Vis. Sci. 49 (2008) 320–332.
[12] W. Zhang, M.R. Prausnitz, A. Edwards, J. Control. Release 99 (2004) 241–258.
[13] M.M. Hermann, A.M. Bron, C.P. Creuzot-Garcher, M. Diestelhorst, J. Glaucoma 20 (2011) 502–508.
[14] D.L. Budenz, Ophthalmology 116 (2009) S43–S47.
[15] J.C. Tsai, Curr. Opin. Ophthalmol. 17 (2006) 190–195.
[16] C. Baudouin, A. Labbe, H. Liang, A. Pauly, F. Brignole-Baudouin, Prog. Retin. Eye Res. 29 (2010) 312–334.
[17] M.L. Becker, N. Huntington, A.D. Woolf, Pediatrics 123 (2009) E305–E311.
[18] D.-M. Anaya, M. Kwak, A.J. Musser, K. Müllen, A. Herrmann, Chem. Eur. J. 16 (2010) 12852–12859.
[19] K.-M. Song, M. Cho, H. Jo, K. Min, S.H. Jeon, T. Kim, M.S. Han, J.K. Ku, C. Ban, Anal. Biochem. 415 (2011) 175–181.
[20] L. Jiang, A. Majumdar, W. Hu, T.J. Jaishree, W. Xu, D.J. Patel, Structure 7 (1999) 817–827.
[21] M. Kwak, I.J. Minten, D.-M. Anaya, A.J. Musser, M. Brasch, R.J.M. Nolte, K. Müllen, J.J.L.M. Cornelissen, A. Herrmann, J. Am. Chem. Soc. 132 (2010) 7834–7835.
[22] M. Schultheiss, K. Januschowski, H. Ruschenburg, C. Schramm, S. Schnichels, P. Szurman, K.U. Bartz-Schmidt, M.S. Spitzer, Graefes Arch. Clin. Exp. Ophthalmol. 251 (2013) 1613–1619.
[23] K. Nakano, Y. Terabayashi, A. Shiroma, M. Shimoji, H. Tamotsu, N. Ashimine, S. Ohki, M. Shinzato, K. Teruya, K. Satou, T. Hirano, Genome Announc. 3 (2015) e00932–15.
[24] L.G. Rahme, E.J. Stevens, S.F. Wolfort, J. Shao, R.G. Tompkins, F.M. Ausubel, Science 268 (1995) 1899–1902.
[25] E.J. Lee, D.J. Evans, S.M. Fleiszig, Invest. Ophthalmol. Vis. Sci. 44 (2003) 5220–5227.
[26] N. Cole, M. Krockenberger, F. Stapleton, S. Khan, E. Hume, A.J. Husband, M. Willcox, Infect. Immun. 71 (2003) 1328–1336.
[27] S.K. Lai, Y.Y. Wang, J. Hanes, Adv. Drug Deliv. Rev. 61 (2009) 158–171.
[28] D.A. Norris, P.J.J. Sinko, Appl. Polym. Sci. 63 (1997) 1481–1492.
[29] R.J. Weber, S.I. Liang, N.S. Selden, T.A. Desai, Z.J. Gartner, Biomacromolecules 15 (2014) 4621–4626.
[30] N.S. Selden, M.E. Todhunter, N.Y. Jee, J.S. Liu, K.E. Broaders, Z.J. Gartner, J. Am. Chem. Soc. 134 (2012) 765–768.
[31] S. Schnichels, M. Schultheiss, J. Hofmann, P. Szurman, K.U. Bartz-Schmidt, M.S. Spitzer, Neurochem. Int. 60 (2012) 581–591.
[32] M. Schultheiss, S. Schnichels, K. Miteva, K. Warstat, P. Szurman, M.S. Spitzer, S. Van Linthout, Graefes Arch. Clin. Exp. Ophthalmol. 250 (2012) 1221–1229.
[33] M.A. Dobrovolskaia, S.E. McNeil, Nat. Nanotechnol. 2 (2007) 469–478.
[34] Y. Diebold, M. Calonge, Prog. Retin. Eye Res. 29 (2010) 596–609.
[35] R. Stoltenburg, C. Reinemann, B. Strehlitz, Biomol. Eng. 24 (2007) 381–403.
[36] L. Gold, B. Polisky, O. Uhlenbeck, M. Yarus, Annu. Rev. Biochem. 64 (1995) 763–797.
[37] S. Duench, L. Sorbara, N. Keir, T. Simpson, L. Jones, Optom. Vis. Sci. 90 (2013) 546–556.
[38] A. Niiya, N. Yokoi, Y. Matsumoto, A. Komuro, T. Ishibashi, S. Tomii, J. He, S. Kinoshita, Ophthalmologica 214 (2000) 332–336.
[39] A. Lux, S. Maier, S. Dinslage, R. Suverkrup, M. Diestelhorst, Br. J. Ophthalmol. 87 (2003) 436–440.
[40] A. Steinfeld, A. Lux, S. Maier, R. Suverkrup, M. Diestelhorst, Br. J. Ophthalmol. 88 (2004) 48–53.
[41] D. Tognetto, P. Cecchini, G. Sanguinetti, M. Pedio, G. Ravalico, J. Cataract. Refract. Surg. 27 (2001) 1392–1396.
[42] T.N. Yusifov, A.R. Abduragimov, K. Narsinh, O.K. Gasymov, B.J. Glasgow, Mol. Vis. 14 (2008) 180–188.
[43] K.H. Cheng, S.L. Leung, H.W. Hoekman, W.H. Beekhuis, P.G. Mulder, A.J. Geerards, A. Kijlstra, Lancet 354 (1999) 181–185.
[44] S.M. Fleiszig, E.J. Lee, C. Wu, R.C. Andika, V. Vallas, M. Portoles, D.W. Frank, CLAO J. 24 (1998) 41–47.
[45] J.G. Souza, K. Dias, T.A. Pereira, D.S. Bernardi, R.F.J. Lopez, Pharm. Pharmacol. 66 (2014) 507–530.
[46] F. Lallemand, O. Felt-Baeyens, K. Besseghir, F. Behar-Cohen, R. Gurny, Eur. J. Pharm. Biopharm. 56 (2003) 307–318.
[47] S.Y. Liu, L. Jones, F.X. Gu, Macromol. Biosci. 12 (2012) 608–620.
[48] R.C. Nagarwal, P.N. Singh, S. Kant, P. Maiti, J.K. Pandit, Chem. Pharm. Bull. 59 (2011) 272–278.
[49] R.S. Bhatta, H. Chandasana, Y.S. Chhonker, C. Rathi, D. Kumar, K. Mitra, P.K. Shukla, Int. J. Pharm. 432 (2012) 105–112.
[50] E. Vega, F. Gamisans, M.L. Garcia, A. Chauvet, F. Lacoulonche, M.A.J. Egea, Pharm. Sci. 97 (2008) 5306–5317.
[51] A. Bochot, E. Fattal, J. Control. Release 161 (2012) 628–634.